Available online at www.sciencedirect.com

SCIENCE DIRECT®

Journal of the Mechanics and Physics of Solids
54 (2006) 1093–1119

JOURNAL OF THE MECHANICS AND PHYSICS OF SOLIDS

www.elsevier.com/locate/jmps

Deflections of a rubber membrane ☆

A.P.S. Selvadurai*,[1]

Department of Civil Engineering and Applied Mechanics, McGill University, 817 Sherbrooke Street West, Montreal, Que., Canada H3A 2K6

Received 28 October 2005; received in revised form 3 January 2006; accepted 4 January 2006

Abstract

This paper deals with the problem of the transverse deflection of a natural rubber membrane that is fixed along a circular boundary. Uniaxial experiments were performed in order to characterize the constitutive behaviour of the rubber material in terms of several constitutive models available in the literature. These constitutive models were used to develop computational estimates for the quasi-static load–displacement response of a rigid spherical indentor that deflects the rubber membrane in a controlled fashion and to determine the deflected shape of the membrane at specified load levels. Both axisymmetric and asymmetric deflections of the rubber membrane were investigated. The paper provides a comparison of the experimental results for the membrane deflections with results derived from computational simulations.

Keywords: Constitutive models for rubber; Rubber membranes; Indentation of rubber membranes; Computational modeling; Indentation experiments on rubber membranes

1. Introduction

Modern developments in the mechanics of rubber-like materials commence with the seminal works of R.S. Rivlin, which are presented in the collective works edited by Barenblatt and Joseph (1997). The contributions to the theory of elastic materials exhibiting large strain phenomena, subsequent to Rivlin's work, are far too numerous to

☆In memory of Ronald Samuel Rivlin (1915–2005).

*Tel.: +1 514 398 6672; fax: +1 514 398 7361.
E-mail address: patrick.selvadurai@mcgill.ca.
[1]William Scott Professor and James McGill Professor.

0022-5096/$ - see front matter
doi:10.1016/j.jmps.2006.01.001

be cited individually; complete accounts of these developments are given in the review and survey articles by Doyle and Ericksen (1956), Rivlin (1960), Adkins (1961) and Spencer (1970) and in the volumes by Green and Adkins (1970), Treloar (1975, 1976), Carlson and Shield (1980), Ogden (1984), Lur'e (1990), Truesdell and Noll (1992) and Drozdov (1996). Recent developments in the theory of non-linear elasticity are given in the noteworthy survey volume by Fu and Ogden (2001) and in the lectures series organized by Hayes and Saccomandi (2001) and Saccomandi and Ogden (2004). The mechanics of rubber-like membranes is an area of application that has aided developments in the theory of finite elasticity; problems related to the *in-plane* homogeneous straining of rubber membranes are given in the classical studies by Rivlin and Saunders (1951), while the work of Gent and Rivlin (1952) deals with the inflation, extension and torsion of a cylindrical rubber tube. Plane deformations of neo-Hookean membranes were investigated by Wong and Shield (1969) who showed that under large meridional strains the non-linear problem can be reduced to a linear problem.

A further class of problems deals with edge-supported membranes that can experience large deformations and large strains as a result of loads applied in a transverse direction. This topic, of general interest to the study of the mechanics of membranes, plates and shells, commenced with the works of Föppl, Hencky, Clebsch, Schwerin, Girkmann, von Karman and others. Useful historical reviews are given by Timoshenko (1953), Timoshenko and Woinowsky-Krieger (1959), Naghdi (1972), Libai and Simmonds (1998) and Steigmann (2001). An early application of the theory of finite elasticity to study the inflation of a membrane is given by Adkins and Rivlin (1952), who considered the inflation of a plane sheet of rubber to a nearly spherical shape. In their study, the experimental results of Treloar (1944) were complemented by a comprehensive finite elasticity analysis of the problem for various rubber-like elastic materials, with different forms of the strain energy functions. Klingbeil and Shield (1964) used a central difference analysis of the pressurized flat circular rubber membrane problem to determine the empirical forms of the relevant strain energy functions. Foster (1967) examined a similar problem related to the inflation of a flat circular membrane to a nearly spherical shape, and presented comparisons with analytical solutions developed for a neo-Hookean material. The problem of the stress concentration due to stretching a rubber sheet containing either a circular hole or a rigid circular inclusion was examined by Yang (1967); numerical results were presented for a rubber-like elastic material with a strain energy function of the Mooney–Rivlin type. Hart-Smith and Crisp (1967) presented a very comprehensive study of the stretching of a rubber membrane and the theoretical developments were discussed in relation to the experimental results obtained by Treloar (1944). These authors also highlighted the advantage of using the membrane inflation problem as a technique for determining the constitutive parameters of rubber-like materials. Wu (1970a) considered the problem of the deformation of a tube of hyper-elastic material that transforms the tube to an annulus and presented an exact solution to the problem, applicable to hyper-elastic materials with strain energy functions of the Mooney–Rivlin and neo-Hookean types. Wu (1971) also applied these methodologies to examine certain two-dimensional contact problems associated with the indentation of a pressurized cylindrical membrane. Kydoniefs and Spencer (1969) and Kydoniefs (1969) examined, respectively, hyper-elastic problems related to the behaviour of an initially axisymmetric cylindrical membrane and the interaction of an initially cylindrical membrane enclosing a rigid body. Of related interest is the paper by Pipkin (1968) who considered solutions to hyper-elastic membrane problems where the undeformed surface corresponds to a cylindrical surface. In this case, the equation of equilibrium for the direction tangent to the meridian curve can be integrated exactly. Further integrable forms of the equations for a membrane are given by Wu (1970b). Solutions to a class of deformations associated with non-planar rubber-like membranes have also been presented by Wu (1972, 1974, 1979); references to further studies in this area are given by Spencer (1970). Yang and Feng (1970) examined the problem of the inflation of a flat circular membrane due to uniform pressure. The numerical technique proposed in the paper was used to develop solutions for the inflation of both a circular membrane and a sheet of rubber, the constitutive behaviour of which was modelled by a Mooney–Rivlin material, with extensive numerical results provided for the membrane profile at different stages of the inflation process. The problem of the axisymmetric indentation of a circular membrane by a spherical indentor was examined by Yang and Hsu (1971); again, the governing non-linear equations were solved for a Mooney–Rivlin material. The membrane indentation problem discussed in the paper by Yang and Hsu (1971) closely resembles the axisymmetric study discussed in the present paper. Further results were obtained by Feng and Yang (1973), Yang and Lu (1973), Feng et al. (1974), and Feng and Huang (1975) for inflation and inflation-induced contact problems related to both circular and rectangular membranes. Problems related to the axisymmetric inflation of a circular membrane containing a rigid disc inclusion and the inflation of an ellipsoidal membrane were examined by Tielking and Feng (1974), using a minimum potential energy approach. Feng et al. (1974) extended these studies to develop a solution to the problem of an edge-constrained square membrane subjected to uniform pressure and included a situation where a contact constraint is induced by a rigid immovable smooth obstacle interacting with the deforming membrane. The problem of radial deformation related to a plane-sheet containing either a circular hole or a rigid circular inclusion was examined by Verma and Rana (1978). The measure of strain used in their study is that of Seth (1964) and the solution differs from that given by Yang (1967). Naghdi and Tang (1977) present a comprehensive study of the problem of controllable deformations possible in elastic membranes and provide a wide range of general theorems applicable to thin shells composed of both compressible and incompressible hyper-elastic materials. Pujara and Lardner (1978) discuss the inflation problem for a flat circular membrane and present results for two classes of rubber-like elastic materials, including the Mooney–Rivlin material and one suitable for blood cell membranes proposed by Skalak et al. (1973). Wu (1979) examined the finite strain elasticity problem related to a membrane; the treatment in the paper was relatively general, although explicit results were given for the problem of a plane circular membrane of a neo-Hookean material that transformed into a near-spherical shape. Feng (1987) examined the problem of the indentation of a membrane by an indentor in the form of a paraboloid of revolution, giving numerical results for the case where a square membrane composed of a Mooney–Rivlin material is subjected to indentation. The study by Fulton and Simmonds (1986) considered the large deformations resulting from edge loading of annular membranes. Results were presented for hyper-elastic materials with strain energy functions of the neo-Hookean and Mooney–Rivlin forms and for the strain energy function proposed by Rivlin and Saunders (1951). The problem of the finite deformation of a circular elastic membrane containing an axially loaded concentric rigid inclusion was considered by Tezduyar et al. (1987); a Newton–Raphson technique was used to solve the resulting non-linear problem for the special case of a Mooney–Rivlin material. Pamplona and Bevilacqua (1992) considered a similar problem for both neo-Hookean and Mooney–Rivlin materials, and the resulting non-linear problem was solved using a numerical scheme based on the Picard-iteration technique. The problem of finite deformation and stability of spherical membranes under axisymmetric concentrated loads has been investigated, both experimentally and computationally, by Glockner and Vishwanath (1972), Szyszkowski and Glockner (1987) and Dacko and Glockner (1988). Non-linear problems arising as a result of ponding instabilities in membranes due to fluid accumulation are discussed by Tuan (1998). The analysis presented by Li and Steigmann (1995) considers the point loading of a spherical elastic membrane with a relaxed strain energy function derived from the three-term strain energy function given by Ogden (1972). Useful experimental results concerning nano-indentation of polymeric surfaces are given by Poilane et al. (2000), although the results are largely related to the linear elastic analysis of the indentation problem. The study by Begley and Mackin (2004) also considers the indentation of a circular membrane in the context of a large deflection theory and provides additional references to similar investigations. The inflation of a rubber-like elastic material was examined by Rachik et al. (2001) giving a useful account of the use of the experimental results for the purposes of material parameter identification, both directly and indirectly, for strain energy functions of the following forms: the generalized Mooney–Rivlin and the van der Waals models, and those proposed by Ogden (1972), Yeoh (1993) and Arruda and Boyce (1993). A computational treatment of the pressurized response of hyper-elastic membranes with general boundary configurations was given by de Souza Neto et al. (1995). Arroyo and Belytschko (2002) examined the finite deformation problem for a membrane in the context of the modelling of nano-tubes; in their study, a continuum model was presented for a one-atom thick crystalline film. An inter-atomic potential of the Born-type was used to construct the strain energy function applicable to the equivalent continuum. These authors have implemented the constitutive model in an advanced computational scheme that can accommodate large strain elasticity phenomena. Computational results presented illustrate the development of global and local instabilities in nano-tubes. Finally, Steigmann (2005) has investigated the problem of the puncturing of a rubber membrane by a loaded blunt frictionless indentor, obtaining a solution for the conditions under which a circular hole is formed at the centre of the contacting membrane.

This overview is not meant to be complete; the review article by Beatty (1987) and the volumes by Green and Adkins (1970), Truesdell and Noll (1992) and Libai and Simmonds (1998) contain further references to topics of interest to the membrane problems. Other aspects of membrane behaviour include the development of instabilities in the form of wrinkling and local buckling; the volume by Antman (1995) and the articles by Haughton (2001) and Steigmann (2001) can be consulted for more complete discussions of these topics.

This paper first presents an experimental study of the uniaxial response of a natural rubber for the purposes of establishing the most appropriate form of the constitutive relationship to describe its hyper-elastic behaviour. Correlations with uniaxial test data are used to characterize the constitutive response of the rubber material in terms of the hyper-elastic models described by the Mooney–Rivlin, neo-Hookean, Blatz–Ko, Yeoh and Ogden forms. The experimental work is extended to determine both the axisymmetric and asymmetric responses of a membrane that is fixed along a circular boundary and subjected to transverse indentation by a rigid spherical indentor. The frictional characteristics of the contact between the indentor and the rubber membrane are also evaluated experimentally.

The constitutive models developed through uniaxial testing are implemented in a standard computational code to predict the indentational response of a rubber membrane both in terms of the load–displacement response of the rigid spherical indentor and the deflected shape of the membrane. The computational modelling also takes into consideration the influence of friction between the rigid indentor and the rubber membrane. The predictive capabilities of the constitutive models are examined through a comparison of the experimental results and computational predictions for both the load–displacement response of the indentor and through an examination of the deflected shape of the membrane.

2. Uniaxial testing of the rubber material

The uniaxial testing of the rubber material was carried out using an experimental device that maintained the ends of the sample in a constrained fixed condition, preventing, lateral contraction during extension. This is a particularly convenient testing arrangement provided the constitutive parameter identification is restricted to the data taken from the region of the sample that exhibits a near homogeneous strain. The nominal overall dimensions of the sample used in the uniaxial testing were 70 mm in length and 90 mm in width (Fig. 1). An added novel feature in the testing introduced cuts in the sample to create three test specimens within the same test, with nominal cross-sectional dimensions of each sample being $30.0\,\text{mm} \times 2.0\,\text{mm}$. The overall load–displacement response of the tested specimen is thus a combination of the response from each ligament. To ensure minimal slip or damage an additional piece of a hard rubber was glued to the grip regions of the test specimen using a non-reactive instant adhesive. The specially fabricated steel grips enabled the application of an aligned load without the development of either an eccentricity or a tilt of the test specimen. The grips were mounted directly on the platforms of a servo-controlled MTS machine (Fig. 1), where the upper set of grips could be operated in a displacement control mode at a specified rate. Since the specimen was highly flexible in comparison to the rigid steel grips and the test frame, the application of a machine stiffness correction to the measured deformations was considered to be unnecessary. Calibration of the relative displacement of the grips indicated that, for relative displacements smaller than 30 mm relative movement of the grip heads agreed closely with the average reading of two LVDTs located on either side of the test specimen. As the specimen was stretched, the

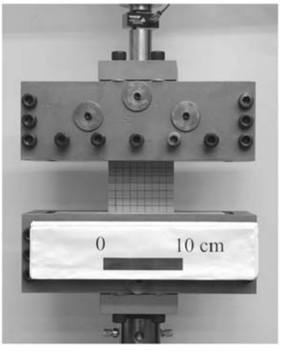

Fig. 1. Experimental setup.

accuracy of the LVDTs diminished significantly, particularly at large displacements; therefore for simplicity and accuracy, the movement of the grips was taken as the change in the current gauge length l. Despite the constraining effects of the grips at very large axial strains, a significant part of the sample was subjected to homogeneous straining (Fig. 2). The initial length of the specimen $l_0 = 70\,\text{mm}$ was taken as the initial gauge length. The nominal stress σ_0 is defined as the value of total load, measured by the load cell, divided by three initial areas of cross-section for each test element. The strain ε_0 is calculated as the percentage change in the *initial* gauge length. All experiments were performed at a constant uniaxial strain-rate $\dot{\varepsilon}_0$, defined by

$$\dot{\varepsilon}_0 = \frac{\mathrm{d}}{\mathrm{d}t}\left(\frac{l - l_0}{l_0}\right). \tag{2.1}$$

The experiments were performed in a Materials Testing Laboratory, where the room temperature was approximately 22 °C. The results of the uniaxial tests conducted up to failure of one or more ligaments are shown in Fig. 2. The experiments were performed at two different strain-rates, 114 and 28.5%/min. The experimental results show reasonable repeatability between sets of experiments, within the range of accuracy of the tests. These

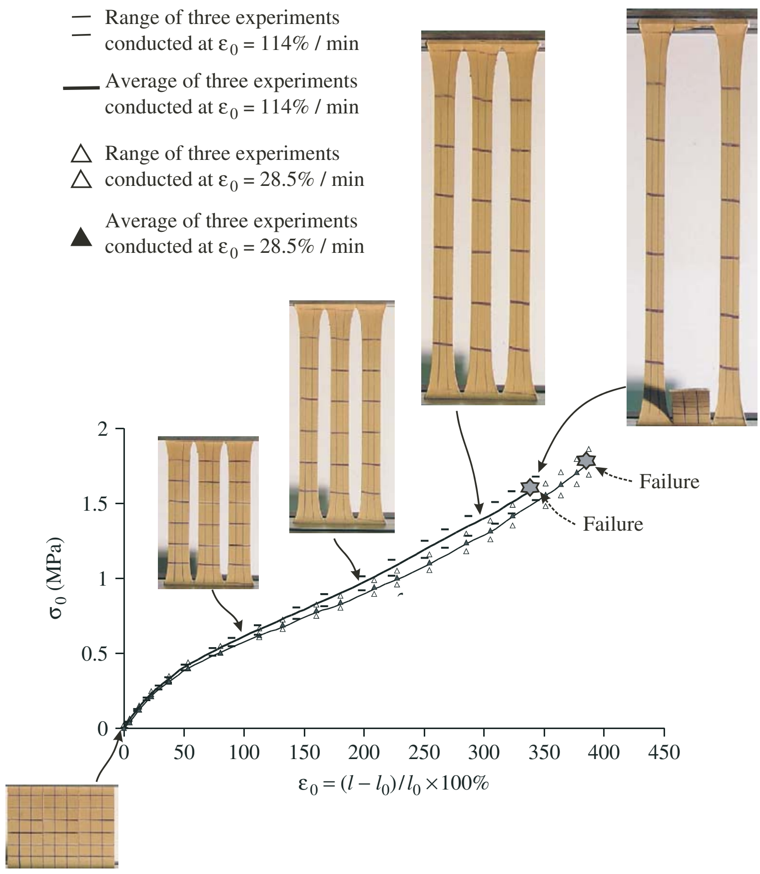

Fig. 2. Mechanical behaviour of a rubber during uniaxial stretching.

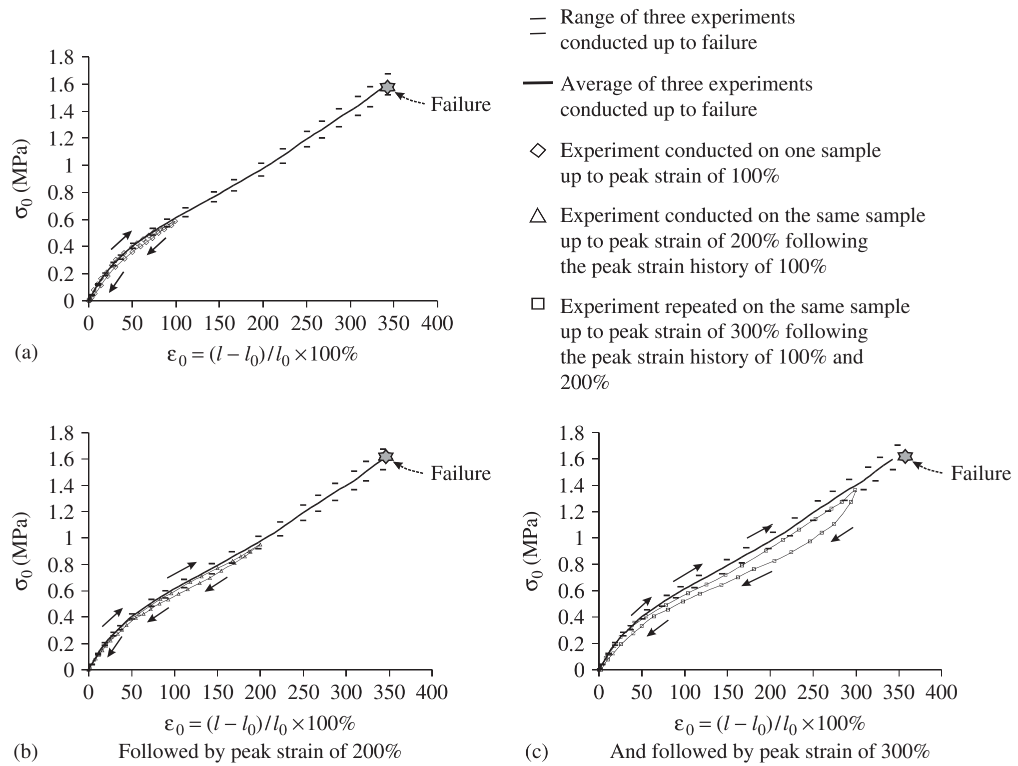

Fig. 3. Uniaxial response of a sample subjected to three loading–unloading cycles at different peak strains: (a) loading–unloading cycle up to peak strain of 100%; (b) followed by peak strain of 200%; and (c) followed by peak strain of 300%.

tests also indicate that the variation of strain-rate has little or no influence on the measured uniaxial responses. Test results indicate that the effects of the fixity constraints were negligible, particularly when the strain was very large (e.g. $\varepsilon_0 > 150\%$). Further experiments were conducted to observe the influence of the peak strain on any irreversible deformations of the rubber. In these tests, the *same* specimen was subjected to three cycles of loading–unloading stress histories. The peak strain at each loading–unloading cycle, however, varied from 100% to 200% to 300%. The results are presented in Fig. 3. It was observed that hysteretic or Mullins-type effects (i.e. the loading path differs from an unloading path; see e.g. Mullins, 1947, 1969; Johnson and Beatty, 1993, 1995; Beatty, 2001a; Ogden, 2004; Dorfmann and Ogden, 2004) were almost negligible at peak strains up to both 100% and 200%. Evidence of hysteresis in the stress–strain paths materialized only at peak strains of 300% and even in this case virtually no permanent strains were observed during complete unloading of the test specimens.

3. Development of constitutive models

The modelling of the constitutive behaviour of hyper-elastic rubber-like materials that are characterized by large strain responses and by the absence of irreversible strains during loading–unloading cycles has been extensively researched since the seminal works of Treloar, Rivlin, Saunders and others. There are a number of constitutive models of hyper-elastic behaviour available in the literature and no attempt will be made here to provide a complete review. In addition to the classical literature in finite elasticity (Green and Adkins, 1970; Treloar, 1975, 1976; Truesdell and Noll, 1992) the reader is referred to Deam and Edwards (1976), Ogden (1984), Lur'e (1990), Drozdov (1996), Dorfmann and Muhr (1999), Boyce and Arruda (2000), Fu and Ogden (2001), Besdo et al. (2001), Busfield and Muhr (2003) and Saccomandi and Ogden (2004) for in-depth reviews of the extensive range of constitutive models proposed to describe hyper-elastic responses of rubber-like materials. The objective here is to use the uniaxial test data to establish parameters for a set of constitutive models that are used quite extensively to model the hyper-elastic behaviour of rubber-like materials. The choice of the models, including Mooney–Rivlin, neo-Hookean, Blatz–Ko, Yeoh and Ogden type, is also dictated by their availability in a documented and validated computational code; this will ultimately be used to examine the mechanics of the transverse indentation of a membrane characterized by the same constitutive responses. All the constitutive models employed in the calibration exercise were applicable to incompressible elastic materials. The parameter evaluations were performed using the results of the strains applicable to the region of the test specimens that underwent near homogeneous straining. The validity of the incompressibility assumption was assessed by examining the lateral contraction of the membrane specimen during monotonic uniform stretching. It was observed that the strain ratios corresponded to a near incompressibility condition characterized by a third invariant, which had a value of approximately 0.97–0.99. (It is explicitly assumed that, during stretching, the lateral contractive strain in the thickness direction of the specimen was identical to the lateral contractive strain over the width of the specimen.) The parameters thus determined were also assessed in terms of their ability to accurately match the stress–strain responses over a large range of strains.

3.1. Mooney–Rivlin model

This is the classical form of the strain energy function (Mooney, 1940; Rivlin, 1948; Spencer, 2004) applicable to incompressible elastic materials ($I_3 = 1$) and assumes a linear dependency in the first and second strain invariants (I_1 and I_2) associated with the deformed state, i.e.,

$$W = C_1(I_1 - 3) + C_2(I_2 - 3), \tag{3.1}$$

where C_1 and C_2 are constants. They are also related to the linear elastic shear modulus (G) through the relationship $G = 2(C_1 + C_2)$. Within the stretch range $\lambda(= 1 + \varepsilon_0) \in [1.2, 2.3]$, the relation between $\sigma_0/[2(\lambda - 1/\lambda^2)]$ (where σ_0 is the nominal stress) and $1/\lambda$ is linear; the slope of the line gives the value of C_2 and the intercept (as $\lambda^{-1} \to 0$) gives the value of C_1. Using the experimental data for the axial stretch and the nominal stress and using a least-squares technique for obtaining a line of best fit, we obtain the following values for the parameters governing the Mooney–Rivlin form of the constitutive model: $C_1 = 0.1361\,\text{MPa}$ and $C_2 = 0.0806\,\text{MPa}$. Using these values a good theoretical representation is achieved (see Fig. 4) for strains up to $\varepsilon_0 = 150\%$. It can also be shown that the Mooney–Rivlin form of the strain energy function is adequate for describing the mechanical behaviour of rubber-like elastic materials that undergo moderately large deformations that can be described by a second-order theory of elasticity

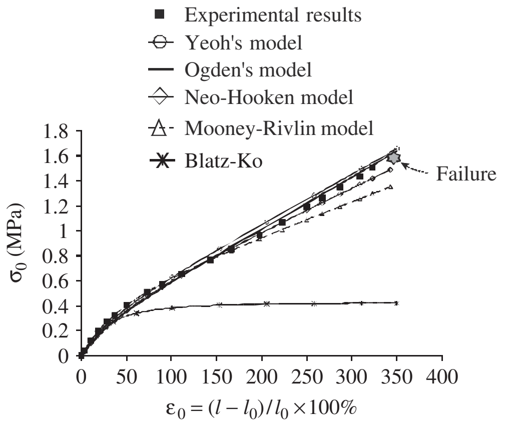

Fig. 4. Model representations of the experimental data by various models.

(Rivlin, 1953; Green and Spratt, 1954; Green and Adkins, 1970; Selvadurai and Spencer, 1972; Selvadurai, 2002).

3.2. Neo-Hookean model

The neo-Hookean form of strain energy function is a special case of the Mooney–Rivlin form of strain energy function when $C_2 = 0$, i.e.,

$$W = C_1(I_1 - 3). \tag{3.2}$$

The single parameter can be determined using a procedure similar to that described above, except that the intercept is determined, so that there is a good match between the nominal stress–stretch plot for a wider range of values of the stretch. It is found that the best fit for the nominal stress vs. strain does not result in the best fit for the plot of $\sigma_0/[2(\lambda - 1/\lambda^2)]$ vs. $1/\lambda$. The best match (see Fig. 4) between the nominal stress vs. strain data over the strain range $\varepsilon_0 < 150\%$ is obtained when $C_1 \approx 0.17\,\text{MPa}$. A further observation is that, whereas the Mooney–Rivlin form of strain energy function gives a good match with the experimental results at strains $\varepsilon_0 < 150\%$, the neo-Hookean model gives a better correlation at larger strains.

3.3. Blatz–Ko model

Using results of experimental investigations on *compressible* rubber-like materials, Blatz and Ko (1962) proposed a strain energy function that has a dependency on the second and third strain invariants (I_2 and I_3), i.e.,

$$W = \frac{G}{2}\left(\frac{I_2}{I_3} + 2\sqrt{I_3} - 5\right), \tag{3.3}$$

where G is the linear elastic shear modulus. For an incompressible elastic material, $I_3 = 3$, and the Blatz–Ko form of the strain energy function reduces to

$$W = \frac{G}{2}(I_2 - 3). \tag{3.4}$$

Considering the experimental data presented earlier, the shear modulus of the rubber-like material used in the experimental investigation is $G(=2\{C_1+C_2\})=0.4334\,\text{MPa}$, with $C_1=0.1361\,\text{MPa}$ and $C_2=0.0806\,\text{MPa}$. We note the fact that the Blatz–Ko model was developed with applications to compressible materials in mind; with incompressible elastic materials, the dependence of the constitutive response on the single parameter G effectively constrains the Blatz–Ko model, in the sense that there is little flexibility in the form of the constitutive relationship to match the experimental data for the nominal stress vs. strain over a wide range of strains. The results for the nominal stress vs. stretch data are shown in Fig. 4; it is evident that the Blatz–Ko model can only accurately capture the mechanical response up to strains within the range, $\varepsilon_0=40\%$.

3.4. Yeoh model

The constitutive model for incompressible hyper-elastic rubber-like materials proposed by Yeoh (1993) assumes that the strain energy function is independent of the second strain invariant and can be represented as a power series in terms of the variable (I_1-3), i.e.,

$$W=\sum_{i=1}^{N}\tilde{C}_i(I_1-3)^i, \tag{3.5}$$

where N is the number of terms in the series, $\tilde{C}_i$ are constants and, for a single term in the series, the Yeoh model reduces to the neo-Hookean form. As observed previously, the neo-Hookean model slightly underestimates the uniaxial stress–stretch response for the rubber, particularly for strains $\varepsilon_0>150\%$. The higher-order terms in the series (3.5) offer a possibility of obtaining a better match with the experimental data over a wider range of strains. For example, considering only powers of (I_1-3) up to the second order, the value of $\tilde{C}_1=0.15\,\text{MPa}$ is chosen such that it is slightly smaller than the elastic parameter of C_1 applicable to the neo-Hookean model and the value of $\tilde{C}_2$ is then chosen such that the model gives an acceptable match with the experimental results for strains in the range $\varepsilon_0>150\%$; this yields $\tilde{C}_2=0.003\,\text{MPa}$. Fig. 4 shows the model duplication of the experimental results. The constitutive relationship proposed by Yeoh (1993) therefore gives a better match than the models discussed previously.

3.5. Ogden model

The strain energy function proposed by Ogden (1972) is based on the experimental results for rubber-like materials obtained by Treloar (1944). The versatility of the model in matching experimental data over a wide range of strains is well-established. The model has a sufficient number of parameters that can be experimentally determined to achieve impressive correlations with experimental data. Ogden's (1972) model assumes that the strain energy function can be represented in terms of three principal stretches $\lambda_i\ (i=1,2,3)$, in the form

$$W=\sum_{i=1}^{N}\frac{2\tilde{\mu}_i}{\alpha_i^2}\left(\lambda_1^{\alpha_i}+\lambda_2^{\alpha_i}+\lambda_3^{\alpha_i}-3\right), \tag{3.6}$$

where N, $\tilde{\mu}_i$ and α_i are material parameters. The values of $\tilde{\mu}_i$ are related to the linear elastic shear modulus G through the consistency condition

$$\sum_{i=1}^{N} \tilde{\mu}_i = G. \tag{3.7}$$

For purposes of comparison, we choose $N = 1$, such that, when $\alpha_1 = 2$, the strain energy function (3.6) reduces to that for the neo-Hookean model (3.2), which slightly underestimates the stress–strain response in the strain range $\varepsilon_0 > 150\%$. We therefore need to choose a slightly larger value of $\alpha_1 = 2.1$ for the Ogden model in order to obtain a better match at higher strains. Using a least-squares approach, the best fit with the experimental data is obtained when the value of the shear modulus $G \approx 0.29$ MPa. The matching of the experimental data with the model proposed by Ogden (1972) is shown in Fig. 4. As is evident, the Ogden model provides a better representation with the experimental data over a wide range of strains. In summary, a comparison of the experimental results and model duplications by various models is presented in Fig. 4; the experimental data for the uniaxial response of the rubber material can be accurately represented by the constitutive models proposed by Yeoh (1993) and Ogden (1972). Although the Mooney–Rivlin and neo-Hookean forms of the strain energy functions tend to slightly underestimate the stress–strain response, particularly at strains $\varepsilon_0 > 150\%$, they are able to duplicate reasonably well the overall uniaxial stress–strain response of the rubber. The strain energy function proposed by Blatz and Ko (1962) has limited capability in accurately modelling the uniaxial stress–strain response for a wide range of strains; satisfactory correlation with this model is obtained only up to a maximum strain of approximately $\varepsilon_0 = 40\%$. All five strain energy functions will, however, be retained in the computational evaluations of the axisymmetric membrane indentation problem. Also it is noted that the extraction of the parameters governing these strain energy functions is done in a direct way involving a least-squares approach and no other constraints are invoked. Numerous other constitutive models for hyper-elastic rubber-like materials are available in the literature. For example, Beatty (2001b) and Hill (2001) have presented, respectively, authoritative studies of Bell- and Varga-type hyper-elastic materials. The computational implementations of these constitutive models are, however, lacking.

4. Frictional contact between brass and rubber

The basic problem examined in this paper relates to the transverse indentation of an edge-supported rubber membrane by a rigid spherical indentor (Fig. 5). The load–displacement response of the indentor is influenced not only by the constitutive characteristics of

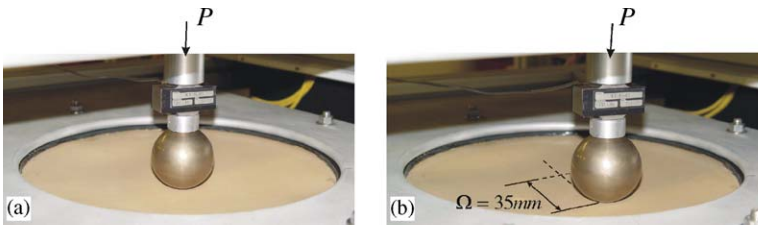

Fig. 5. Indentation of the rubber membrane: (a) axisymmetric indentation, and (b) asymmetric indentation.

the membrane material but also the nature of the contact between the metallic indentor and the rubber. The frictional contact between rubber-like materials and solid surfaces is influenced by a number of factors including the constitutive behaviour of the rubber material itself, the surface roughness characteristics of both the rubber and the solid surface, molecular attraction and interfacial adhesion between the surfaces, the rate of relative movement between the surfaces and the influence of chemicals and impurities at the contacting zones (Singer and Pollack, 1992; Pooley and Tabor, 1972; Persson, 1998a, b). The topic of frictional behaviour of rubber-like materials in contact with solid surfaces has been the subject of extensive research, commencing with the seminal works of Schallamach (1952, 1953, 1963) and Grosch (1963) who investigated the influence of many of the above factors both experimentally and through the development of plausible models to explain the composition of the frictional response. The fundamental studies by Johnson et al. (1971), Schallamach (1975) and the review articles by Roberts and Thomas (1975), Barquins (1985, 1992, 1993), Roberts (1989) and Persson (1998a, b) contain extensive discussions and further references to the topic of friction development between rubber-like materials and solid surfaces. Much of the literature in this area also focuses on rubber-like materials that contain additives necessary to satisfy functional requirements of the rubber. The presence of additives alters the hyper-elastic behaviour, giving rise to dominant rate-dependency effects that are not present in most pure rubber-like materials. The rubber used in the current experimental investigations shows almost negligible rate-dependent effects and hysterisis in the stress–strain behaviour at moderate to large strains. The objective of this phase of the study was to take into account, in a phenomenological manner, the nature of frictional contact between the metallic material used for the indentor and the rubber material. The models available for the description of frictional phenomena between materials are many and varied and attention was restricted to identifying the material parameters that would allow the modelling of frictional contact by appeal to the classical Coulomb friction model. Even in this case, determination of the frictional characteristics is non-routine and has to consider the surface roughness characteristics of the indentor, the rate-sensitivity of the frictional contact and the magnitude of the normal stress in relation to the stresses required to induce large strains or even failure in the rubber material. The friction experiments discussed in the ensuing were conducted to obtain a global value for the Coulomb friction characteristics of contact between the metallic material and the rubber. The experimental investigations commenced with the initiation of contact between a brass plate of prescribed roughness and the membrane material that is bonded to a rigid surface. The thickness of the contacting brass plate was kept to a minimum (9.5 mm) in order to reduce the influence of overturning moments that can materialize during shear movement of the plate. The plan dimensions of the brass plate were $127\,\mathrm{mm} \times 127\,\mathrm{mm}$ and the contact between the plate and the bonded rubber membrane material was established by applying a static weight of 100 N. Calculations indicated that the plate was able to initiate contact with virtually no flexural deformations of the plate. The surface texture of the brass plate was highly polished with a maximum asperity difference of 0.75 μm between any two locations within the contact region. This degree of roughness corresponded to the roughness characteristics of the highly polished brass sphere that was used in the membrane indentation tests. The metallic plate was attached with an inextensible cable (length 254 mm) to a computer controlled electro-mechanical actuator that could be pre-programmed to apply a constant rate of relative displacement. The general layout of the experimental configuration is illustrated in Fig. 6.

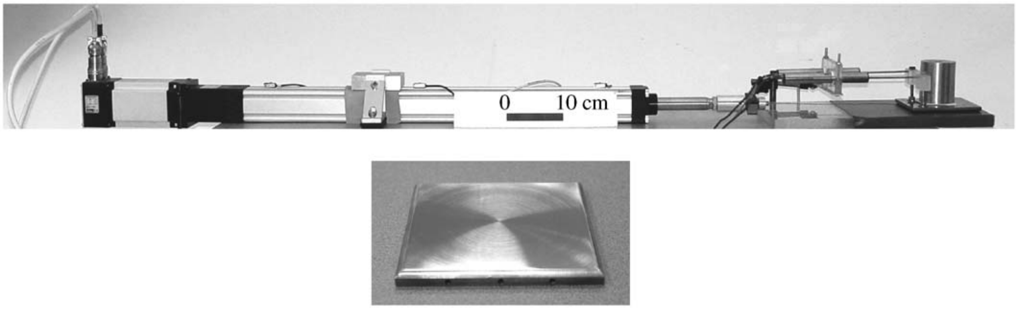

Fig. 6. Experimental configuration used for measurement of friction properties between rubber and a polished brass plate.

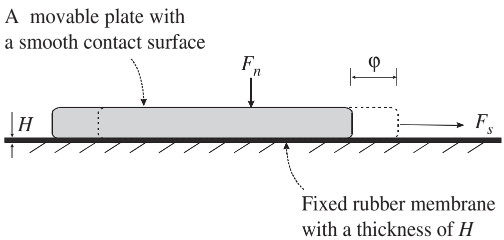

Fig. 7. Schematic view of the experimental arrangement for friction measurement.

The frictional load was measured with a load cell and the relative movement between the plate and the rubber was measured using two displacement transducers (LVDTs) located at the ends of the plate, enabling the assessment of possible rotations of the plate during the application of the shear displacement. Since the contact area remained stationary during the application of the relative shear displacement φ, the coefficient of Coulomb friction at any level of relative shear can be evaluated by considering the ratio between the static normal load (F_{n}) and the applied shear force (F_{s}) (Fig. 7). The relative movement of the rigid plate φ, was measured to within an accuracy of 0.025 mm. During the test, the sliding speed $\dot{\varphi}$ was maintained constant. Observations reported in the literature indicate that the friction properties between metal surfaces and rubber-like materials can be influenced by the speed of the relative movement (Schallamach, 1953; Grosch, 1963; Persson, 1998a). For this reason, the friction characteristics were examined at three rates of relative movement, i.e., $\dot{\varphi} = 0.0254$, 0.254 and 12.7 mm/s. The results obtained from the friction experiments are shown in Fig. 8. The friction loads are mobilized as the shear displacement increases and maintain almost constant values at large relative displacements. The classic "*slip-stick*" phenomena could be observed at the high rates of relative movement, which lead to a significant reduction in the mobilized shear forces. These results also indicate that the average friction coefficient between the brass surface and the rubber membrane was almost *independent* of the rate of relative movement $\dot{\varphi}$ between the brass plate and the rubber material. To further verify this observation, additional friction experiments covering a wider range of rates of relative movement were conducted; the results of these investigations are shown in Fig. 9. It can be observed that the measured

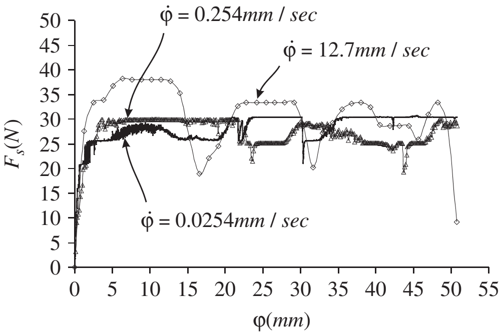

Fig. 8. Frictional behaviour between a brass plate and the rubber (under a normal pressure of $\sigma_n = 1.81$ kPa, F_s the frictional force, and φ the relative displacement between brass plate and rubber membrane).

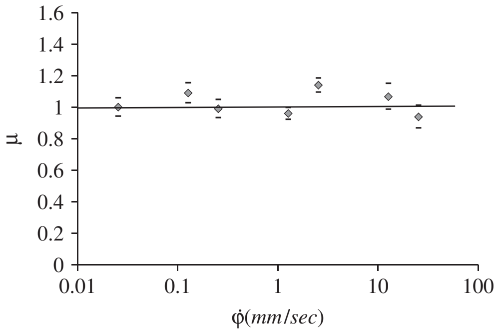

Fig. 9. Influence of the rate of relative movement on the coefficient of Coulomb friction.

coefficient of Coulomb friction is approximately, $\mu = 1.0$, which is applicable to the range $\dot{\varphi} \in [0.0254,\ 25.4\,\text{mm/s}]$. This coefficient was used in the computational modelling.

5. Indentation of the rubber membrane

The membrane testing facility (Fig. 10) was designed to apply a transverse indentational displacement to a membrane of arbitrary shape that is maintained in a fixed condition along a circular boundary. The brass indentor had a spherical shape with a polished surface and was attached to an electro-mechanical actuator that could be pre-programmed to induce a prescribed quasi-static displacement at a given rate. The rubber membrane used in the investigation had a diameter of 250 mm and a thickness of 0.5 mm. The fixity at the boundary was achieved by clamping the membrane between two aluminium plates. To minimize stress concentration effects at the clamped boundary, the aluminium plates used for clamping were provided with a rounded cross-section. To further enhance the fixity condition at the clamped boundary, an additional layer of a PVC material was attached to the rubber membrane using a non-reactive adhesive. This additional layer was provided at the boundary of the clamped edge (Fig. 10b). Experience with testing other polymeric materials indicated that the incorporation of the additional layer eliminates slippage

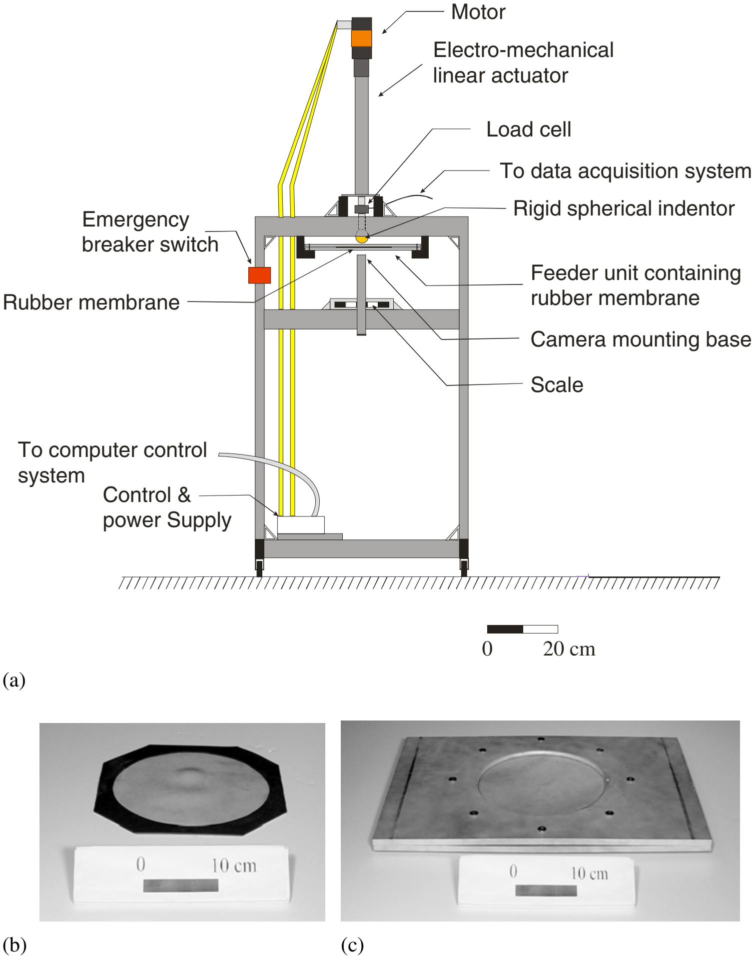

(a)

(b) (c)

Fig. 10. The membrane indentation test facility: (a) apparatus for the membrane indentation tests; (b) the rubber membrane specimen; and (c) the feeder unit containing the rubber.

between the membrane and the aluminium plate and acts to reduce possible stress concentrations near the clamping edge, which could lead to localized failure or tearing of the rubber membrane, particularly at large strains. The feeder unit containing the rubber specimen (Fig. 10c) was placed within a guiding track that enabled the positioning of the indentor contact at any location within the membrane region. During indentation the contact between the rubber membrane and the polished brass sphere was initiated either at the centre of the membrane (Fig. 5a) or at an off-axis location (Fig. 5b). Since the indentational loads were relatively small, the flexibility of the testing system was neglected and the indentational displacement was measured to within ± 0.025 mm. An important aspect of the experimentation involved the determination of the deflected profile of the membrane during different stages of the indentation process. The deflected shape of the membrane was recorded photographically and image analysis of the photographic record was performed to determine quantitative estimates for the deflected shape. The digital camera was rigidly mounted on the test frame and located 1500 mm from the central plane of the test specimen. The deflected shapes of the membrane applicable either to the (r, z) plane or the (x, z) plane were determined using an image analysis technique as described by Klette et al. (1998). Briefly, the images were first measured in units of image pixels and these were calibrated against two scales that were aligned on a line passing through the image plane and normal to the axis of the digital camera. The scales were located on either side of membrane and situated equidistant from the centre of the membrane. The force induced during displacement of the membrane was monitored using a load cell with capacity of 4000 N (1000 lbs). The indentation behaviour was examined by applying the displacements in an incremental manner up to a maximum indentor displacement of $\Delta_{\max} = 127\,\text{mm}$ (5 in.), followed by unloading at the same displacement rate. The displacements were applied in a quasi-static fashion to eliminate any dynamic effects associated with the experimentation. During the axisymmetric indentation experiment, the ratio of the indentor displacement (Δ) to the diameter (d) of the membrane (Δ/d) reached a maximum value of 0.61, which corresponds to a maximum strain of approximately 40% in the r-direction, with assumptions of zero slip at the boundary of the membrane. Typical deflection patterns observed during axisymmetric indentation of the rubber membrane are shown in Fig. 11. The experimental results for the load–displacement behaviour showed excellent repeatability and absence of any noticeable irreversibility due to frictional effects at the membrane–indentor interface. The inset plates in Fig. 11 illustrate the recovery configuration of the membrane upon release of the applied load and there appears to be no

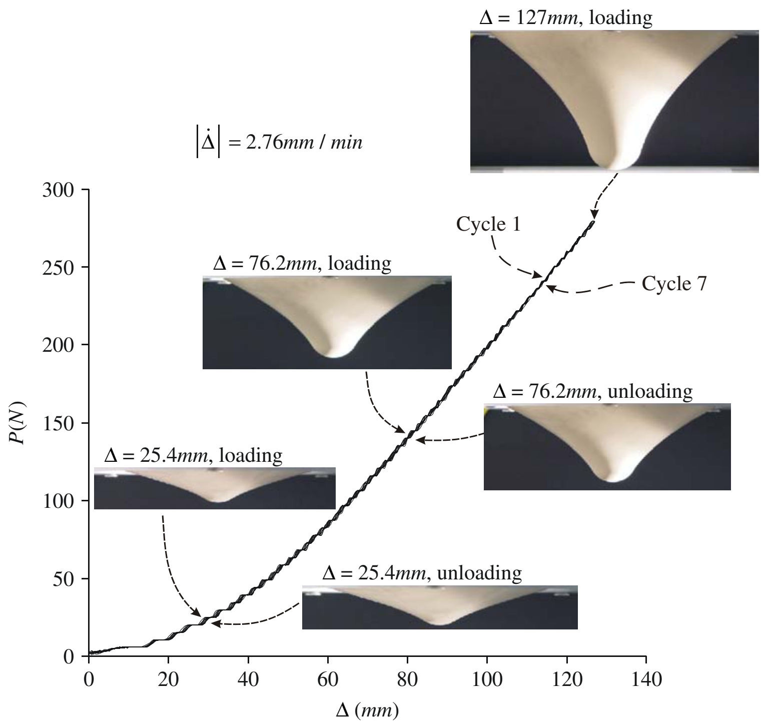

Fig. 11. Deflection of the rubber membrane during axisymmetric indentation.

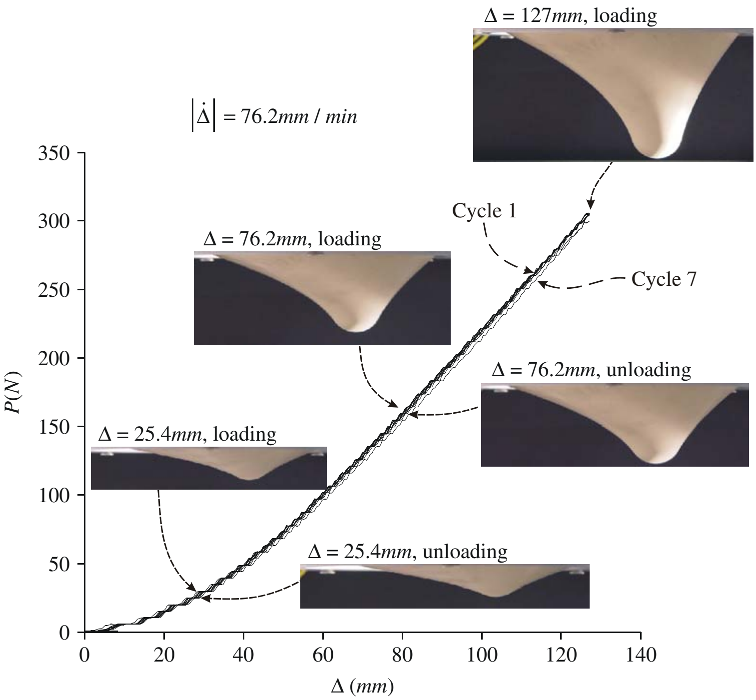

Fig. 12. Deflections of the rubber membrane during asymmetric indentation.

appreciable irreversible deformation after completion of seven cycles of loading and unloading. During asymmetric indentation, the contact between the spherical rigid indentor and the rubber membrane was initiated at a distance of $\Omega = 35$ mm from the axis of symmetry (Fig. 5b). In this test, at a maximum indentor displacement of $\Delta_{\max} = 127$ mm (5 in.), the maximum strain reached was approximately 70% in the x-direction. Typical deflection patterns at various stages of the indentation process are shown in inset photographs of Fig. 12. Again, the experimental results show excellent repeatability and absence of any hysterisis in the load–displacement responses.

6. Computational implementation and comparisons

One of the earliest applications of the finite-element technique to the modelling of rubber-like materials is that of Oden and Sato (1967) who examined the problems related to both in-plane loading of a rectangular membrane fixed along two opposite edges and the transverse loading of a circular membrane fixed at the boundary. The constitutive equations used in their analysis were the Mooney–Rivlin and neo-Hookean types, and the computational results compare quite accurately with results for membrane problems given by Green and Adkins (1970). Applications of the computational approach to the solution of problems in hyper-elasticity are many and varied; recent examples are those by de Souza Neto et al. (1995), Jiang and Haddow (1995) and Verron and Marckmann (2001, 2003), with references to further studies given in the volumes by Zienkiewicz and Taylor (2000) and Belytschko et al. (2000). In the present study, the computational modelling of axisymmetric and asymmetric indentation of the circular rubber membrane with a fixed edge was conducted using the general-purpose finite-element code ABAQUS/Standard (2004). This code is very versatile and has the following features: firstly, all the hyper-elastic constitutive equations characterized by the strain energy function of interest to the material modelling are standard features in the computational approach. Secondly, the code provides a contact algorithm that allows the incorporation of Coulomb friction effects at the advancing contact between the hyper-elastic membrane and the indenting rigid sphere; in the specific case of hyper-elastic materials, the accuracy of the computational code has been adequately verified through comparisons with both exact and approximate results applicable to membrane problems. Finally, the iterative computational algorithms applicable to non-linear problems associated with hyper-elastic materials, frictional phenomena at interfaces and non-stationary (advancing) contact problems are well-documented in terms of both exposition fundamental equations, the associated variational principles as well as the numerical implementation. To the author's knowledge, there are no known analytical solutions, exact or otherwise, that examine simultaneously the non-linear processes associated with hyper-elasticity, Coulomb friction and non-stationary contact. Furthermore, unlike problems related to pressurization of membranes, the presence of frictional contact with an advancing contact region makes the analytical solution of even the axisymmetric membrane indentation problem a non-trivial exercise in the theory of non-linear ordinary differential equations and moving boundary problems. For this reason, recourse can only be made to a computational approach to study the membrane indentation problem. The ABAQUS/Standard code has provisions for the incorporation of a variety of element types for modelling the membrane region. The membrane indentation problem was subjected to preliminary analysis using both a quadratic triangular membrane element (element type-3M6) and a linear solid triangular prism element (element-type C3D6). There were no noticeable differences between the two types of elements. In view of the simultaneous application of the frictional contact algorithm and the advancing contact at a membrane surface, the use of a solid triangular membrane element is expected to lead to better overall accuracy, particularly in identifying the location of slip, contact and separation zones. The contact conditions between the indentor and the membrane were chosen as standard hard contact in the ABAQUS/Standard code. The boundary conditions and mesh discretization applicable to the computational models are shown in Figs. 13a and 14a. Typical deflected configurations of the membrane during indentation by the rigid sphere are shown in Figs. 13b and 14b. The load–displacement relationships obtained via computational modelling of the axisymmetric indentation of the membrane that incorporate the strain energy functions given in Section 3 are shown in Figs. 15a and b for contact Coulomb friction values of 0 and 1, respectively. The analogous results obtained from the experiments involving asymmetric indentation of the membrane are shown in Figs. 16a and b. The general trends in the computational estimates are similar to those observed in the experiments. There are, however, appreciable differences in the magnitudes associated with the load–displacement responses: the closest correlation is achieved with results derived from a strain energy function of the Mooney–Rivlin type. For further evaluation of the accuracy of the predictions from the various constitutive models, we consider the profile of the deflected shapes of the membrane derived at certain load levels. These predictions are obtained by setting the coefficient of friction $\mu = 1$ in the computations. Fig. 17 illustrates comparisons between the computational and the experimental results for the axisymmetric deflected

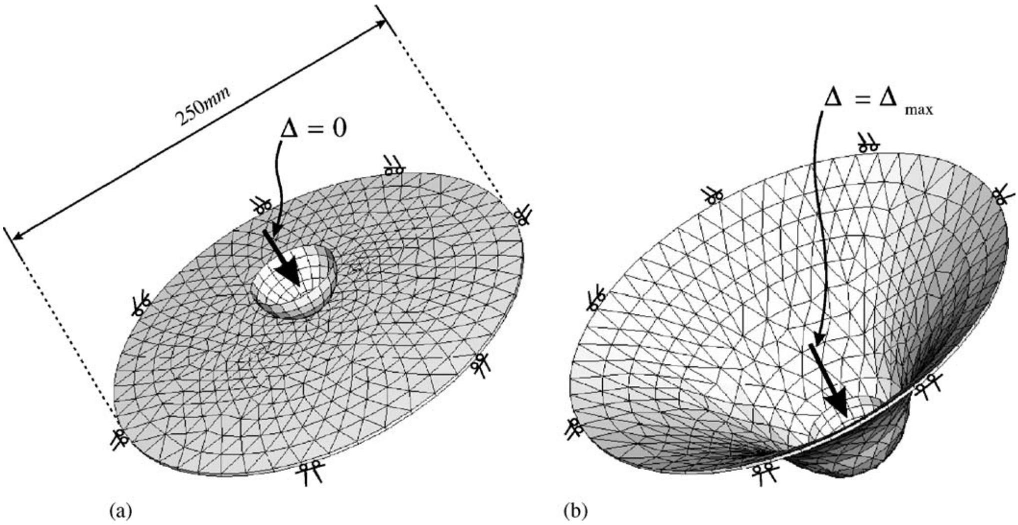

Fig. 13. Axisymmetric indentation of a rubber membrane: (a) mesh configuration and boundary conditions (total number of elements: 816); and (b) deformed shape during maximum indentation.

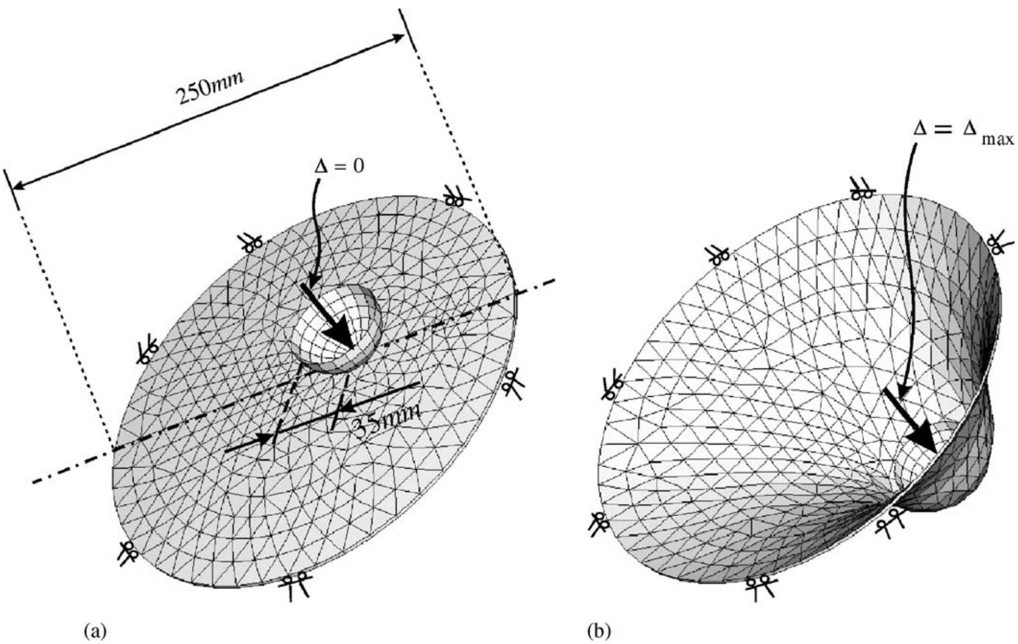

Fig. 14. Asymmetric indentation of a rubber membrane: (a) mesh configuration and boundary conditions (total number of elements: 818); and (b) deformed shape during maximum indentation.

shapes derived from the Mooney–Rivlin, neo-Hookean, Blatz–Ko, Yeoh and Ogden forms for the strain energy function; where applicable, the indentation load levels are chosen as 20, 130 and 280 N. The results derived from the Mooney–Rivlin and Blatz–Ko strain

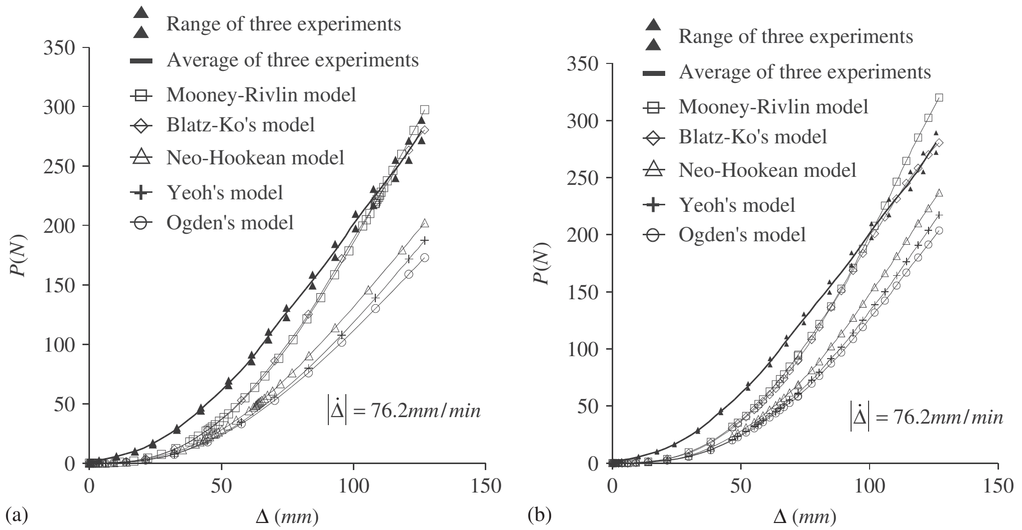

Fig. 15. Load–displacement relationship for the rigid spherical indentor. A comparison of experimental results and computational estimates during axisymmetric indentation: (a) $\mu = 0$ and (b) $\mu = 1.0$.

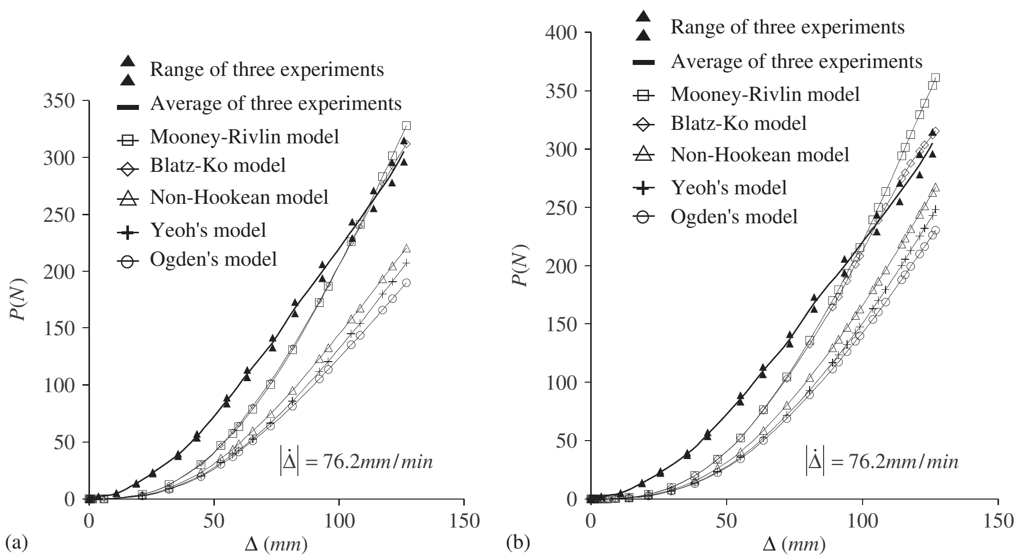

Fig. 16. Load–displacement relationship for the rigid spherical indentor. A comparison of experimental results and computational estimates during asymmetric indentation: (a) $\mu = 0$ and (b) $\mu = 1.0$.

energy functions show the most favourable correlations between the computational and experimental results even though the latter model fared poorly in matching the uniaxial stress–strain response in the large strain range (i.e. $\varepsilon_0 > 50\%$). In the case of results derived from the remaining constitutive models, there is considerable divergence between the

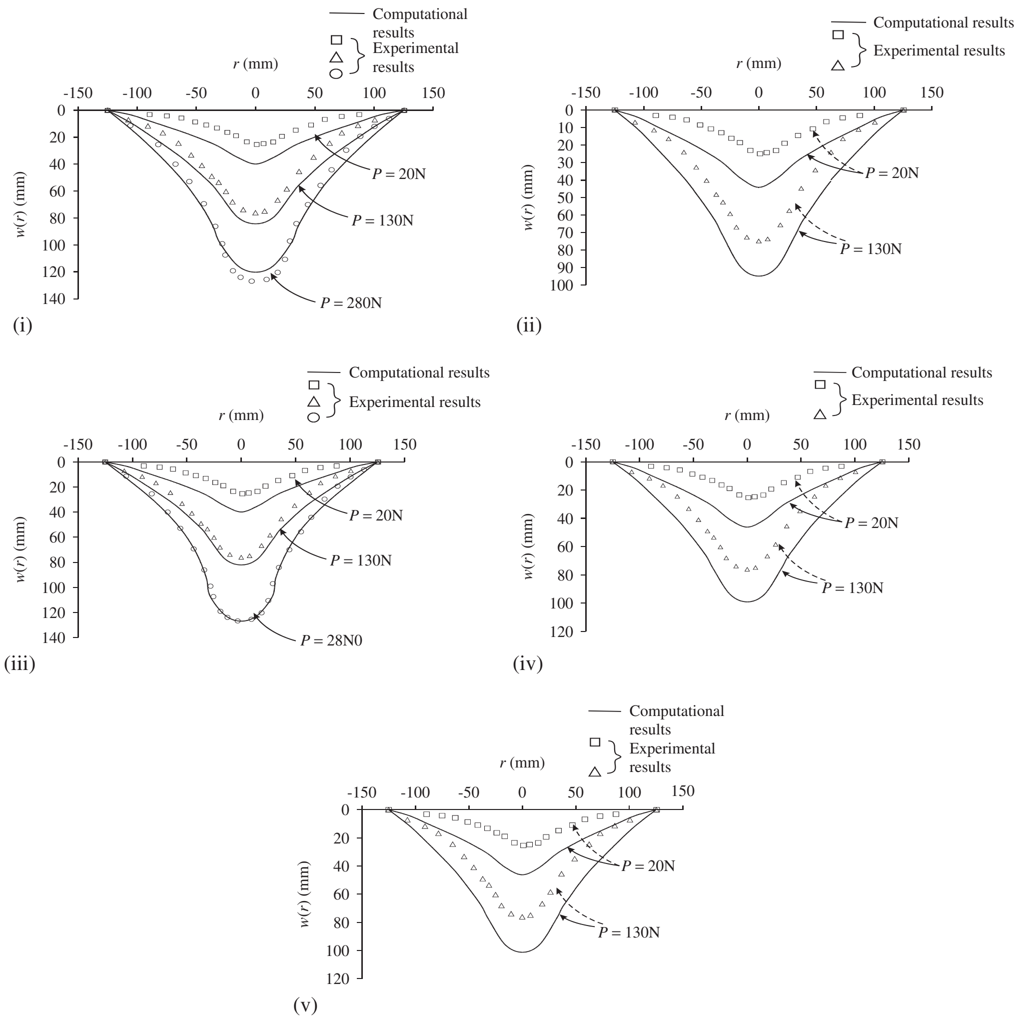

Fig. 17. Comparison of computational predictions and experimental results for the axisymmetric deflection of the rubber membrane: (i) the Mooney–Rivlin model; (ii) the neo-Hookean model; (iii) the Blatz–Ko model; (iv) the Yeoh model; and (v) the Ogden model.

computational predictions and the experimental results at the load level of 280 N. Similar comparisons obtained for the asymmetric indentation of the rubber membrane are shown in Fig. 18, except that in view of the higher loads that are applied, the load levels at which correlations are established are specified at 25, 142 and 305 N. Also, the computational modelling is carried out by setting the coefficient of friction $\mu = 1$. These results indicate the deflection profile along the plane of symmetry of the indentation. The correlations observed are remarkably similar to those associated with the axisymmetric indentation problem, and that the predictions made by the Mooney–Rivlin and Blatz–Ko models offer the closest match.

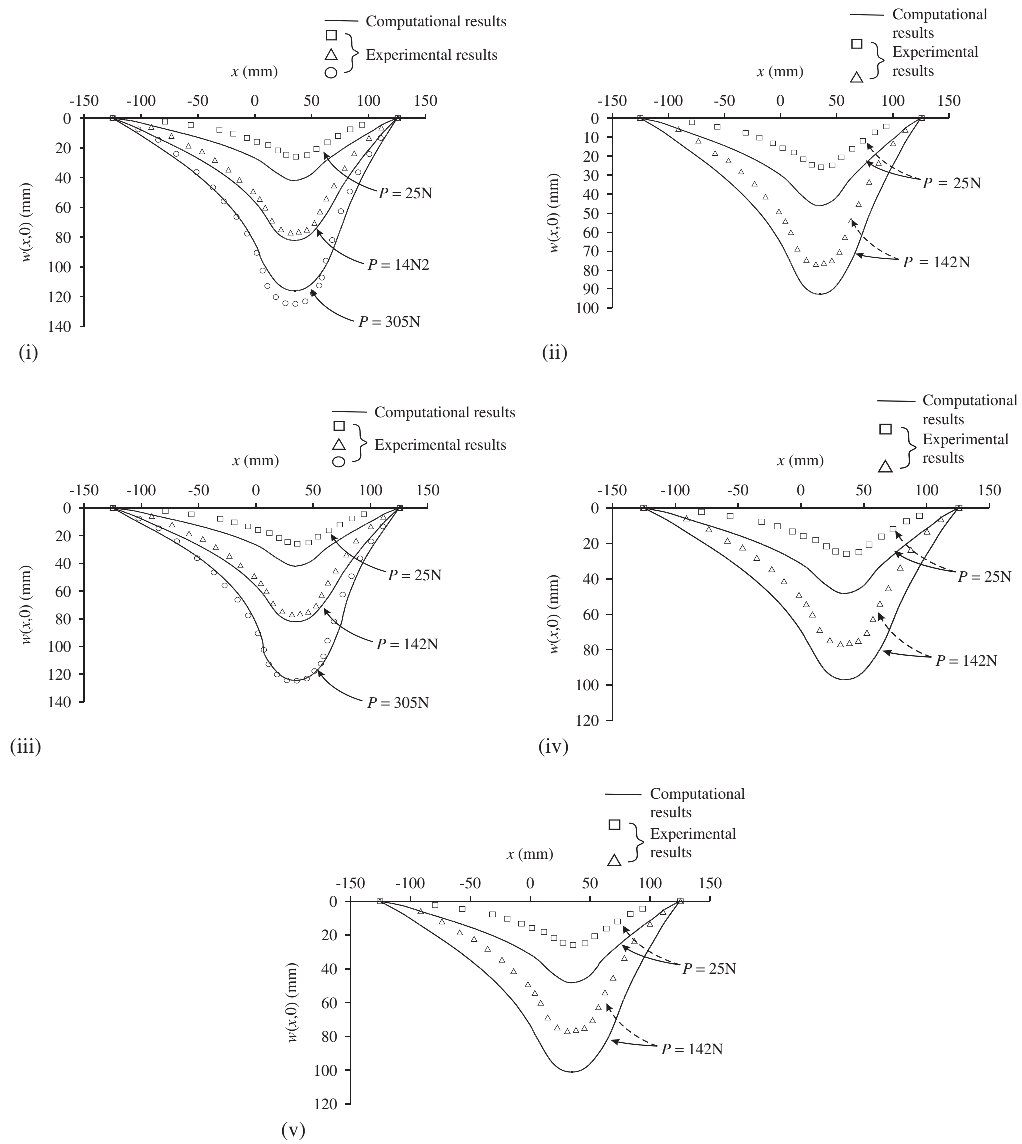

Fig. 18. Comparison of computational predictions and experimental results for the asymmetric deflection of the rubber membrane: (i) the Mooney–Rivlin model; (ii) the neo-Hookean model; (iii) the Blatz–Ko model; (iv) the Yeoh model; and (v) the Ogden model.

7. Conclusions

The modelling of the constitutive behaviour of rubber-like materials continues to be of interest and importance to both materials engineering and continuum solid mechanics. The technological applications of hyper-elastic materials has prompted the development of a wide variety of constitutive models that can be used to describe the mechanical behaviour of rubber-like materials that are void of inelasticity and strain-rate effects. Much of the constitutive characterizations are based on experiments that induce homogeneous states of strain in the test specimens. The correlations established through such exercises suggest that many of the existing models can adequately describe the observed experimental results at both moderate and large strain levels. The current study approaches the validation of the constitutive models developed through uniaxial testing by appeal to an experimentation involving a specific boundary value problem dealing with both axisymmetric and asymmetric transverse indentation of an edge-supported circular membrane. A comparison of the results of experiments and computational predictions indicate that the degree of correlation is not consistent with what is observed in the testing of uniaxial specimens. The results of this research suggest that, even though the indentor induces large deflections of the membrane, the strains encountered in the membrane are still within the moderate range (i.e. $\varepsilon_0 < 70\%$). In these situations the computational estimates that use simpler constitutive models, such as the Mooney–Rivlin and Blatz–Ko types of strain energy functions, provide the best correlations with experimental data. In this sense the selection of a particular form of a strain energy function for either computational or analytical treatment of a problem in rubber elasticity should also give attention to the range of strains that can be experienced in the boundary value problem that is being investigated. Also the model development can be enhanced by consideration of more than one category of experiments.

Acknowledgements

The work described in this paper was supported by the *Max Planck Forschungspreis in the Engineering Sciences* awarded by the Max Planck Gesellschaft, Germany and through a *Discovery Grant* awarded by the Natural Sciences and Engineering Research Council of Canada. The author is grateful to Qifeng Yu for his assistance with the study. The author is grateful to the reviewers for their encouraging and constructive comments.

References

ABAQUS/Standard, 2004. A General-Purpose Finite Element Program, Hibbitt, Karlsson & Sorensen, Inc., Pawtucket, RI, USA.

Adkins, J.E., 1961. Large elastic deformations. In: Sneddon, I.N., Hill, R. (Eds.), Progress in Solid Mechanics, vol. II, pp. 2–60.

Adkins, J.E., Rivlin, R.S., 1952. Large elastic deformations of isotropic materials. 9. The deformation of thin shells. Philos. Trans. Roy. Soc. A 244, 505–531.

Antman, S., 1995. Nonlinear Problems of Elasticity. Springer, Berlin.

Arroyo, M., Belytschko, T., 2002. An atomistic-based finite deformation membrane for single layer crystalline films. J. Mech. Phys. Solids 50, 1941–1977.

Arruda, E.M., Boyce, M.C., 1993. A three-dimensional constitutive model for the large stretch behaviour of rubber elastic materials. J. Mech. Phys. Solids 41, 389–412.

Barenblatt, G.I., Joseph, D.D. (Eds.), 1997. Collected Papers of R.S. Rivlin, vol. I. Springer, Berlin.

Barquins, M., 1985. Sliding friction of rubber and Schallamach waves—a review. Mater. Sci. Eng. 73, 45–63.

Barquins, M., 1992. Adherence, friction and wear of rubber-like materials. Wear 18, 87–117.

Barquins, M., 1993. Friction and wear of rubber-like materials. Wear 160, 1–11.

Beatty, M.F., 1987. Topics in finite elasticity: hyperelasticity of rubber, elastomers, and biological tissues—with examples. Appl. Mech. Rev. 40, 1699–1734.

Beatty, M.F., 2001a. Seven lectures on finite elasticity. Lecture 7. Stress-softening of rubber-like materials—the Mullins effect. In: Hayes, M., Saccomandi, G. (Eds.), Topics in Finite Elasticity, CISM Courses and Lectures No. 424. Springer, Wien, pp. 31–82.

Beatty, M.F., 2001b. Hyperelastic Bell materials: retrospection, experiment, theory. In: Fu, Y.B., Ogden, R.W. (Eds.), Nonlinear Elasticity—Theory and Applications. Cambridge University Press, Cambridge, pp. 58–96.

Begley, M.R., Mackin, T.J., 2004. Spherical indentation of freestanding circular thin films in the membrane regime. J. Mech. Phys. Solids 52, 2005–2023.

Belytschko, T., Liu, W.-K., Moran, B., 2000. Non-linear Finite Elements for Continua and Structures. Wiley, New York.

Besdo, D., Schuster, R.H., Ihlemann, J. (Eds.), 2001. Constitutive Models for Rubber II. In: Proceedings of the Second European Conference on Constitutive Models for Rubber, Hanover, Germany. A.A. Balkema, Lisse.

Blatz, P.J., Ko, W.L., 1962. Application of finite elastic theory to the deformation of rubbery materials. Trans. Soc. Rheol. 6, 223–251.

Boyce, M.C., Arruda, E.M., 2000. Constitutive models for rubber elasticity: a review. Rubber Chem. Technol. 73, 504–523.

Busfield, J.J.C., Muhr, A.H. (Eds.), 2003. Constitutive Models for Rubber III. In: Proceedings of Second European Conference on Constitutive Models for Rubber, London, UK. A.A. Balkema, Lisse.

Carlson, D.E., Shield, R.T. (Eds.), 1980. Finite Elasticity. In: Proceedings of the IUTAM Symposium, Lehigh University, PA. Kluwer Academic Publishers, The Netherlands.

Dacko, A.K., Glockner, P.G., 1988. Spherical inflatable under axisymmetric loads: another look. Int. J. Non-Linear Mech. 23, 393–407.

Deam, R.T., Edwards, S.F., 1976. The theory of rubber elasticity. Philos. Trans. Roy. Soc. 280, 317–353.

de Souza Neto, E.A., Peric, D., Owen, D.R.J., 1995. Finite elasticity in spatial description: linearization aspects with 3-D membrane applications. Int. J. Numer. Methods Eng. 38, 3365–3381.

Dorfmann, A., Muhr, A. (Eds.), 1999. Constitutive Models for Rubber. A.A. Balkema, Rotterdam.

Dorfmann, A., Ogden, R.W., 2004. A constitutive model for the Mullins effect with permanent set in particle-reinforced rubber. Int. J. Solids Struct. 41, 1855–1878.

Doyle, T.C., Ericksen, J.L., 1956. Nonlinear elasticity. Adv. Appl. Mech. 4, 53–115.

Drozdov, A.D., 1996. Finite Elasticity and Viscoelasticity. World Scientific, Singapore.

Feng, W.W., 1987. Indentation of a plane membrane with a rigid paraboloid. Int. J. Non-Linear Mech. 22, 261–265.

Feng, W.W., Huang, P., 1975. On the general contact problem of an inflated nonlinear plane membrane. Int. J. Solids Struct. 11, 437–448.

Feng, W.W., Yang, W.H., 1973. On the contact problem of an inflated spherical nonlinear membrane. J. Appl. Mech. 40, 209–214.

Feng, W.W., Tielking, J.T., Huang, P., 1974. The inflation and contact constraint of a rectangular Mooney membrane. J. Appl. Mech. 41, 979–984.

Foster, H.O., 1967. Inflation of a plane circular membrane. J. Eng. Ind. 89, 403–407.

Fu, Y.B., Ogden, R.W. (Eds.), 2001. Nonlinear Elasticity—Theory and Applications, London Mathematical Society, Lecture Notes Series 283. Cambridge University Press, Cambridge.

Fulton, J.P., Simmonds, J.G., 1986. Large deformations under vertical edge loads of annular membranes with various strain energy densities. J. Non-Linear Mech. 21, 257–267.

Gent, A.N., Rivlin, R.S., 1952. Experiments on the mechanics of rubber II: the torsion, inflation and extension of a tube. Proc. Phys. Soc. B 65, 487–501.

Glockner, P.G., Vishwanath, T., 1972. On the analysis of non-linear membranes. Int. J. Non-Linear Mech. 7, 361–394.

Green, A.E., Adkins, J.E., 1970. Large Elastic Deformations. Oxford University Press, London.

Green, A.E., Spratt, E.B., 1954. Second-order effects in the deformation of elastic bodies. Proc. Roy. Soc. A 224, 347–361.

Grosch, K.A., 1963. The relation between the friction and viscoelastic properties of rubber. Proc. Roy. Soc. A 274, 21–39.

Hart-Smith, L.J., Crisp, J.D.C., 1967. Large elastic deformations of thin rubber membranes. Int. J. Eng. Sci. 5, 1–24.

Haughton, D.M., 2001. Elastic membranes. In: Fu, Y.B., Ogden, R.W. (Eds.), Nonlinear Elasticity—Theory and Applications. Cambridge University Press, Cambridge, pp. 233–267.

Hayes, M., Saccomandi, G. (Eds.), 2001. Topics in Finite Elasticity, CISM Courses and Lectures No. 424. Springer, Wien.

Hill, J.M., 2001. Exact integrals and solutions for finite deformations of the incompressible Varga elastic materials. In: Fu, Y.B., Ogden, R.W. (Eds.), Nonlinear Elasticity—Theory and Applications. Cambridge University Press, Cambridge, pp. 160–200.

Jiang, L., Haddow, J.B., 1995. A finite element formulation for static axisymmetric deformation of hyperelastic membranes. Comput. Struct. 57, 401–405.

Johnson, K.L., Kendall, K., Roberts, A.D., 1971. Surface energy and the contact of elastic solids. Proc. Roy. Soc. A 324, 301–313.

Johnson, M.A., Beatty, M.F., 1993. A constitutive equation for the Mullins effecting stress controlled uniaxial extension experiments. Continuum Mech. Thermodyn. 5, 83–115.

Johnson, M.A., Beatty, M.F., 1995. The Mullins effect in equibiaxial extension and its influence on the inflation of a balloon. Int. J. Engng. Sci. 33, 223–245.

Klette, R., Karsten, S., Andreas, K., 1998. Computer Vision: Three-dimensional Data from Images. Springer, Singapore.

Klingbeil, W.W., Shield, R.T., 1964. Some numerical investigations on empirical strain energy functions in the large axisymmetric extensions of rubber membranes. J. Appl. Math. Phys. (ZAMP) 15, 608–629.

Kydoniefs, A.D., 1969. Finite axisymmetric deformations of an initially cylindrical elastic membrane enclosing a rigid body. Quart. J. Mech. Appl. Math. 22, 319–331.

Kydoniefs, A.D., Spencer, A.J.M., 1969. Finite axisymmetric deformations of an initially cylindrical membrane. Quart. J. Mech. Appl. Math. 22, 87–95.

Li, X., Steigmann, D.J., 1995. Point loads on a hemispherical elastic membrane. J. Non-Linear Mech. 30, 569–581.

Libai, A., Simmonds, J.G., 1998. The Nonlinear Theory of Elastic Shells. Cambridge University Press, Cambridge.

Lur'e, A.I., 1990. Nonlinear Theory of Elasticity. North-Holland, Amsterdam.

Mooney, M., 1940. A theory of large elastic deformation. J. Appl. Phys. 11, 583–593.

Mullins, L., 1947. Effect of stretching on the properties of rubber. J. Rubber Res. 16, 275–289.

Mullins, L., 1969. Softening of rubber by deformation. Rubber Chem. Technol. 42, 339–362.

Naghdi, P.M., 1972. The theory of shells and plates. In: Flugge, S. (Ed.), Handbuch der Physik, vol. IIa/2. In: Truesdell, C. (Ed.), Mechanics of Solids, vol. II. Springer, Berlin, pp. 425–640.

Naghdi, P.M., Tang, P.Y., 1977. Large deformation possible in every isotropic elastic membrane. Philos. Trans. Roy. Soc. 287, 145–187.

Oden, J., Sato, T., 1967. Finite strains and displacements of elastic membranes by the finite element method. Int. J. Solids Struct. 3, 471–488.

Ogden, R.W., 1972. Large deformation isotropic elasticity—on the correlation of theory and experiment for incompressible rubber-like solids. Proc. Roy. Soc. A 326, 565–584.

Ogden, R.W., 1984. Non-Linear Elastic Deformations. Ellis-Horwood, Chichester.

Ogden, R.W., 2004. Elasticity and inelasticity of rubber. In: Saccomandi, G., Ogden, R.W. (Eds.), Mechanics and Thermomechanics of Rubberlike Solids. CISM Courses and Lectures No. 452. Springer, Wien, pp. 135–185.

Pamplona, D.C., Bevilacqua, L., 1992. Large deformations under axial force and moment loads of initially flat annular membranes. Int. J. Non-Linear Mech. 27, 639–650.

Pipkin, A.C., 1968. Integration of an equation in membrane theory. J. Appl. Math. Phys. (ZAMP) 19, 818–819.

Persson, B.N.J., 1998a. On the theory of rubber friction. Surf. Sci. 401, 445–454.

Persson, B.N.J., 1998b. Sliding Friction: Physical Principles and Applications. Springer, Heidelberg.

Poilane, C., Delobelle, P., Lexcellent, C., Hayashi, S., Tobushi, H., 2000. Analysis of the mechanical behavior of shape memory polymer membranes by nanoindentation, bulging and point membrane deflection tests. Thin Solid Films 379, 156–165.

Pooley, C.M., Tabor, D., 1972. Friction and molecular structure: the behaviour of some thermoplastics. Proc. Roy. Soc. A 329, 251–274.

Pujara, P., Lardner, T.J., 1978. Deformations of elastic membranes—effect of different constitutive relations. J. Appl. Math. Phys. (ZAMP) 29, 315–327.

Rachik, M., Schmidt, F., Reuge, N., Le Maoult, Y., Abbe, F., 2001. Elastomers biaxial characterization using bubble inflation technique. II: numerical investigation of some constitutive models. Polym. Eng. Sci. 41, 532–541.

Rivlin, R.S., 1948. Large elastic deformations of isotropic materials. IV. Further developments of the general theory. Philos. Trans. Roy. Soc. A 241, 379–397.

Rivlin, R.S., 1953. The solution of problems in second-order elasticity. J. Ration. Mech. Anal. 2, 53–81.

Rivlin, R.S., 1960. Some topics in finite elasticity. In: Goodier, J.N., Hoff, N.J. (Eds.), Structural Mechanics: Proceedings of the First Symposium on Naval Structural Mechanics. Pergamon Press, Oxford, pp. 169–198.

Rivlin, R.S., Saunders, D.W., 1951. Large elastic deformations of isotropic materials. VII. Experiments on the deformation of rubber. Philos. Trans. Roy. Soc. A 243, 251–288.

Roberts, A.D., 1989. A guide to estimating the friction of rubber. Rubber Chem. Technol. 65, 673–686.

Roberts, A.D., Thomas, A.G., 1975. The adhesion and friction of smooth rubber surfaces. Wear 33, 45–64.

Saccomandi, G., Ogden, R.W. (Eds.), 2004. Mechanics and Thermomechanics of Rubberlike Solids. CISM Courses and Lectures No. 452. Springer, Wien.

Schallamach, A., 1952. The load dependence of rubber friction. Proc. Phys. Soc. London, Sect. B 65, 657–661.

Schallamach, A., 1953. The velocity and temperature dependence of rubber friction. Proc. Phys. Soc. B 66, 386–392.

Schallamach, A., 1963. A theory of dynamical rubber friction. Wear 6, 375–382.

Schallamach, A., 1975. The frictional contact of rubber. In: de Pater, A.D., Talker, J.J. (Eds.), The Mechanics of Contact between Deformable Bodies, Proceedings of the IUTAM Symposium, Enschede. Delft University Press, Delft, pp. 359–376.

Selvadurai, A.P.S., 2002. Second-order elasticity for axisymmetric torsion: a spheroidal coordinate formulation. In: Croitoro, E. (Ed.), Proceedings of the Second Canadian Conference on Nonlinear Solid Mechanics, Vancouver, vol. 1, pp. 27–49.

Selvadurai, A.P.S., Spencer, A.J.M., 1972. Second-order elasticity with axial symmetry. I. General theory. Int. J. Eng. Sci. 10, 97–114.

Seth, B.R., 1964. Second-order effects in elasticity, plasticity and fluid dynamics. In: Proceedings of the XI International Congress on Applied Mechanics, Munich, Germany, pp. 383–389.

Singer, I.L., Pollack, H.M. (Eds.), 1992. Fundamentals of Friction: Macroscopic and Microscopic Processes. Kluwer Academic Publishers, Dordrecht.

Skalak, R., Tozeren, A., Zarda, R.P., Chien, S., 1973. Strain energy function of red blood cell membranes. Biophys. J. 13, 245–264.

Spencer, A.J.M., 1970. The static theory of finite elasticity. J. Inst. Math. Appl. 6, 164–200.

Spencer, A.J.M., 2004. Continuum Mechanics, third ed. Dover Publishers, London.

Steigmann, D.J., 2001. Elements of the theory of elastic surfaces. In: Fu, Y.B., Ogden, R.W. (Eds.), Nonlinear Elasticity—Theory and Applications. Cambridge University Press, Cambridge, pp. 268–304.

Steigmann, D.J., 2005. Puncturing a thin elastic sheet. Int. J. Non-Linear Mech. 40, 255–270.

Szyszkowski, W., Glockner, P.G., 1987. Spherical membranes subjected to vertical concentrated loads: an experimental study. Eng. Struct. 9, 183–192.

Tielking, J.T., Feng, W.W., 1974. The application of the minimum potential energy principle to nonlinear axisymmetric membrane problems. J. Appl. Mech. 41, 491–496.

Tezduyar, T.E., Wheeler, L.T., Graux, L., 1987. Finite deformation of circular elastic membrane containing a concentric rigid inclusion. Int. J. Non-Linear Mech. 22, 61–72.

Timoshenko, S., 1953. History of Strength of Materials: with a Brief Account of the History of Theory of Elasticity and Theory of Structures. McGraw-Hill, New York.

Timoshenko, S., Woinowsky-Krieger, S., 1959. Theory of Plates and Shells, second ed. McGraw-Hill, New York.

Treloar, L.R.G., 1944. Stress–strain data for vulcanized rubber under various types of deformation. Trans. Faraday Soc. 40, 59–70.

Treloar, L.R.G., 1975. Rubber Elasticity, third ed. Oxford University Press, London.

Treloar, L.R.G., 1976. The mechanics of rubber elasticity. Proc. Roy. Soc. A 351, 301–330.

Truesdell, C., Noll, W., 1992. The Non-Linear Field Theories of Mechanics, second ed. Springer, Berlin.

Tuan, C.Y., 1998. Ponding on circular membranes. Int. J. Solids Struct. 35, 269–283.

Verma, P.D.S., Rana, O.H., 1978. Radial deformation of a plane sheet containing a circular hole or inclusion. Int. J. Non-Linear Mech. 13, 223–232.

Verron, E., Marckmann, G., 2001. An axisymmetric B-spline model for the non-linear inflation of rubber-like membranes. Comput. Methods Appl. Mech. Eng. 190, 6271–6289.

Verron, E., Marckmann, G., 2003. Inflation of elastomeric circular membranes using network constitutive equations. Int. J. Non-Linear Mech. 38, 1221–1235.

Wong, F.S., Shield, R.T., 1969. Large plane deformations of thin elastic sheets of neo-Hookean material. J. Appl. Math. Phys. (ZAMP) 20, 176–199.

Wu, C.H., 1970a. Tube to annulus—an exact non-linear membrane solution. Quart. Appl. Math. 27, 489–496.

Wu, C.H., 1970b. On certain integrable nonlinear membrane solutions. Quart. Appl. Math. 28, 81–90.

Wu, C.H., 1971. On the contact problems of inflated cylindrical membranes with a life raft as an example. J. Appl. Mech. 93, 615–622.

Wu, C.H., 1972. Sphere-like deformations of a balloon. Quart. Appl. Math. 30, 183–194.

Wu, C.H., 1974. Infinitely stretched Mooney surfaces of revolution are uniformly stretched catenoids. Quart. Appl. Math. 33, 273–284.

Wu, C.H., 1979. Large finite strain membrane problems. Quart. Appl. Math. 36, 347–359.

Yang, W.H., 1967. Stress concentration in a rubber sheet under axially symmetric stretching. J. Appl. Mech. 34, 942–946.

Yang, W.H., Feng, W.W., 1970. On axisymmetrical deformations of non-linear membranes. J. Appl. Mech. 37, 1002–1011.

Yang, W.H., Hsu, K.H., 1971. Indentation of a circular membrane. J. Appl. Mech. 38, 227–229.

Yang, W.H., Lu, C.H., 1973. General deformations of neo-Hookean membrane. J. Appl. Mech. 40, 9–12.

Yeoh, O.H., 1993. Some forms of the strain energy function for rubber. Rubber Chem. Technol. 66, 754–771.

Zienkiewicz, O.C., Taylor, R.L., 2000. The Finite Element Method, fifth ed. Butterworth-Heinemann, Oxford.